

Microscopic structure of the discommensurate phases in Ge(111)/Ga. II. Domain superstructure and discommensurations

M. Böhringer,* P. Molinàs-Mata, E. Artacho, and J. Zegehen†

Max-Planck-Institut für Festkörperforschung, Postfach 80 06 65, D-70506 Stuttgart, Germany

(Received 15 July 1994)

We present atomically resolved scanning tunneling microscope (STM) images of two of the discommensurate phases— γ and β —occurring in the system Ge(111)/Ga. In both phases Ga atoms substitute the Ge atoms of the substrate surface layer, resulting in a local (1×1) structure within domains. In the β phase, which occurs at slightly higher Ga coverages than the γ phase, a stacking fault is visible in half of the domains. The domains are separated by elementary discommensurations, so-called domain walls. In the present study we focus on the microscopic structure of these walls—a problem that is hard to access with methods other than STM. From the STM data we deduce a microscopic model of the walls of the β phase, where virtually all dangling bonds are saturated—in contrast to the situation in the γ phase. This energetically favorable situation is enabled by the presence of the stacking fault. We propose that the gain in energy due to the removal of all dangling bonds in the walls of the β phase exceeds the loss in energy associated with the stacking fault, driving the transition from the γ to the β phase.

I. INTRODUCTION

In part I (Ref. 1) of this paper the results of first-principles calculations and x-ray standing wave (XSW) measurements on the three discommensurate phases occurring in the adsorbate system Ge(111)/Ga are presented. They yield a rather complete understanding of these phases in terms of number of Ga atoms per (1×1) -surface unit cell, their position and chemical binding to the substrate as well as the strain in the interior of the domains. However, a complete description of the discommensurate phase also demands specification of domain size and shape as well as the internal structure of the domain walls. Especially, a detailed modeling of the domain boundaries is desirable to understand these phases, because the energetic contributions from the walls may be comparable in size with the other energies defining the overall structure. Indeed we propose that in the system investigated the transition between the two phases, γ and β , is driven by a change in the binding within the domain walls, as will be discussed in the following.

Answers to these questions are beyond the scope of present first-principle methods. Although the XSW results clearly reflect the discommensurate nature of the phases occurring, conclusions on the size and shape of the domains as well as the modeling of the domain walls is difficult or at least ambiguous from XSW alone. Scanning tunneling microscope (STM), however, provides valuable real space information concerning size of the domains, symmetry of the tiling, strain within the domains and the structure of the domain walls. Of course, the results of the *ab initio* calculations and XSW measurements are instrumental for understanding the STM results. For ex-

ample, STM does not directly provide information on the chemical identity of the surface atoms. This, however, can be obtained from XSW measurements and confirmed by calculations. In addition, the contrast in STM images usually originates from geometric as well as electronic contributions, which often are difficult to separate. Thus, a comparison with calculated local densities of electronic surface states might help to evaluate the relative contribution of these two effects to the STM image. This is of importance especially at the domain walls, where both a change in geometry as well as in the electronic structure of the surface is expected.

While the characterization of the discommensurate phases in Ge(111)/Ga in terms of domain size, shape, and symmetry via STM is described elsewhere,² here we emphasize the microscopic, i.e., atomically resolved structure and the comparison with the results obtained in part I. From XSW measurements and *ab initio* calculations it was concluded that in both phases the (1×1) structure of the ideally terminated (111) surface is preserved within the domains, except for a small increase of the lattice constant due to adsorbate induced expansive strain. One Ga atom per (1×1) surface unit cell substitutes the Ge atoms of the substrate surface layer. However, due to rehybridization the substitutional Ga atoms are strongly downward relaxed with respect to regular lattice sites, yielding large compressive stress in the (1×1) structure, which leads to a local lattice expansion and discommensurations (domain walls). The main difference between γ and β phase is a stacking fault in the surface layer in half of the domains of the β phase. The accompanying small loss in energy due to Ga in faulted positions must be overcome by an energetically more favorable situation at the domain walls. To understand the

transition from the γ to the β phase in more detail, we focus in the present STM study on the structure of the domain walls of the γ and the β phase.

II. EXPERIMENT

All STM investigations were performed in an ultra-high vacuum (UHV) system with a base pressure of 10^{-10} mbar, equipped with sample preparation facilities, low-energy electron diffraction (LEED), and Auger electron spectroscopy for surface characterization. Slightly doped Ge single crystals were oriented to (111) ($\pm 0.3^\circ$), cut and Syton polished. Prior to loading in the UHV system the samples were cleaned with organic solvents and oxidized with 30% H_2O_2 . After degassing the sample in UHV the $c(2 \times 8)$ reconstruction of clean Ge(111) was obtained by repeated Ar sputtering at 650°C and $p_{\text{Ar}} \approx 5 \times 10^{-5}$ mbar. On surfaces showing an excellent $c(2 \times 8)$ LEED pattern, Ga was deposited from a thermal effusion cell at a rate of approximately 1 ML/min [1 ML on Ge(111) $\equiv 7.23 \times 10^{14}$ atoms $\text{cm}^{-2} \equiv 1.42 \text{ \AA Ga}$] on the sample at room temperature. The Ga flux was calibrated by a quartz microbalance. Subsequent annealing to 450°C – 500°C was monitored simultaneously by LEED in order to identify the phases and check for homogeneity. For an exact determination of the saturation coverages of the different phases it was important to exclude Ga loss to the bulk that might occur during the preparation. To assure Ga saturation of the bulk, Ga was predeposited on the clean Ge sample. After annealing, the excess of Ga on the surface was removed by a sputter cycle. On thus prepared Ge substrates, the saturation coverages were determined by LEED. The STM images were obtained in the constant current mode at room temperature with a commercially available STM (Ref. 3). The convention used here is that the bias U_g across the tunnel junction is the voltage of the sample measured with respect to the tip.

III. STM RESULTS

A. γ phase

In Fig. 1 STM images of the γ phase of Ge(111)/Ga are shown for different tunneling bias U_g and tunneling currents I_t . At high positive values of U_g and small I_t , a domain superlattice with a periodicity of $\approx 30 \text{ \AA}$ ($29.6 \pm 1.5 \text{ \AA}$) is visible with the domains appearing triangular in shape [Fig. 1(a)]. Higher tunneling currents, i.e., smaller tip-surface distances are required to obtain atomic resolution within the domains [Fig. 1(b)]. On the atomic scale, the domains appear roughly hexagonal with fluctuating size. Within the domains the surface atoms, which are Ga atoms in substitutional positions according to part I, are essentially in (1×1) geometry, however the lattice constant is increased by $\approx 8\%$ (as will be discussed below) with respect to the bulk due to expansive strain. At positive U_g , the domain walls appear as structureless depressions. When changing the polarity of U_g a reversal of the contrast is observed [Fig. 1(c)]. Within the

domains, resolution is poor and only rows can vaguely be identified, whereas corrugation maxima with atomic distances are prominent within the walls. Although the distribution of the maxima appears rather irregular, a triangular arrangement of three maxima is visible as repeating structural element at the wall intersections.

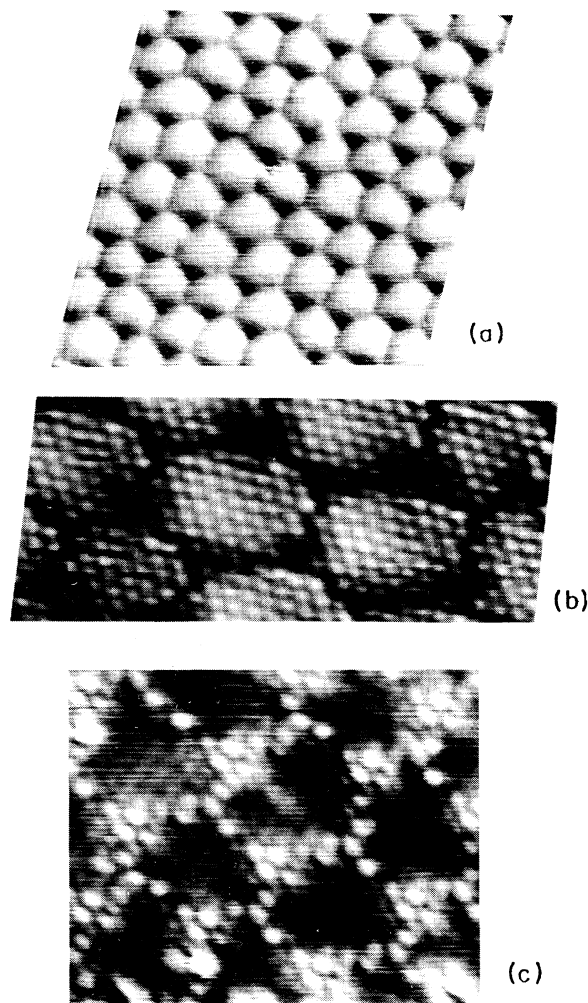


FIG. 1. (a) Domain superlattice of the γ phase at 0.6 ML Ga coverage. The periodicity of the superstructure is $\approx 30 \text{ \AA}$. Two types of wall intersections are visible, leading to trigonal rather than hexagonal symmetry. $U_g = 2.5 \text{ V}$, $I_t = 50 \text{ pA}$, $200 \text{ \AA} \times 200 \text{ \AA}$, weighted differential mode. (b) High resolution STM constant current topograph (CCT) of the domains of the γ phase. Within the domains the surface atoms are in (1×1) geometry with a lattice constant increased by $\approx 8\%$ with respect to the bulk (4.3 \AA and 4.0 \AA , respectively). $U_g = 2.2 \text{ V}$, $I_t = 23 \text{ nA}$, $100 \text{ \AA} \times 45 \text{ \AA}$, weighted differential mode. (c) At negative bias, corrugation maxima are visible within the domain walls, most probably originating from dangling bonds in the second layer. Note the triangular arrangement of maxima at every second wall intersection. $U_g = -2.5 \text{ V}$, $I_t = 2.9 \text{ nA}$, $90 \text{ \AA} \times 90 \text{ \AA}$, weighted differential mode.

B. β phase

Figure 2 reproduces STM images of the β phase at a coverage around 1.0 ML Ga, i.e., slightly above the saturation coverage of this phase (≈ 0.8 ML). Again the domain superstructure is best visible at high positive U_g and small I_t . Figure 2(a) is presented in the weighted differential mode (normalized sum of the image and its gradient) to emphasize the structure above and below a step of the substrate. Noteworthy, the domain walls continue across the step without lateral shift, which indicates a deep penetration of the strain field, caused by the surface discommensurations, into the bulk. Two types of triangular domains are distinguishable, apparently differing in size, which tile the surface in an alternating way. The reason for the inequivalence becomes evident from the atomically resolved image Fig. 2(b). As in the γ phase the surface Ga atoms are in (1×1) geometry within the domains, with the lattice constant increased by $\approx 8\%$. However, the indicated line reveals a stacking fault with respect to the underlying substrate in half

of the domains. The domain wall is shown in more detail in Fig. 2(c). Atomic resolution can also be obtained at negative bias [Fig. 2(d)]. At negative U_g the domain walls are considerably less distinct and most remarkably no stacking fault is observable. When the domain superstructure is imaged at smaller values of I_t , the walls again appear as depressions as is shown in Fig. 3, where the same part of the surface is imaged at positive [Fig. 3(a)] and negative [Fig. 3(b)] bias. At Ga coverages near the transition from the γ to the β phase (0.7–0.8 ML Ga), we observe both phases in coexistence [Fig. 4(a)] allowing a direct comparison of corrugations, domain sizes, and lattice constants [Fig. 4(b)].

IV. DISCUSSION

The basis for our interpretation of the atomically resolved images of the γ and β phase are calculated local densities of occupied and unoccupied surface states (LDOS), obtained from *ab initio* local density approxi-

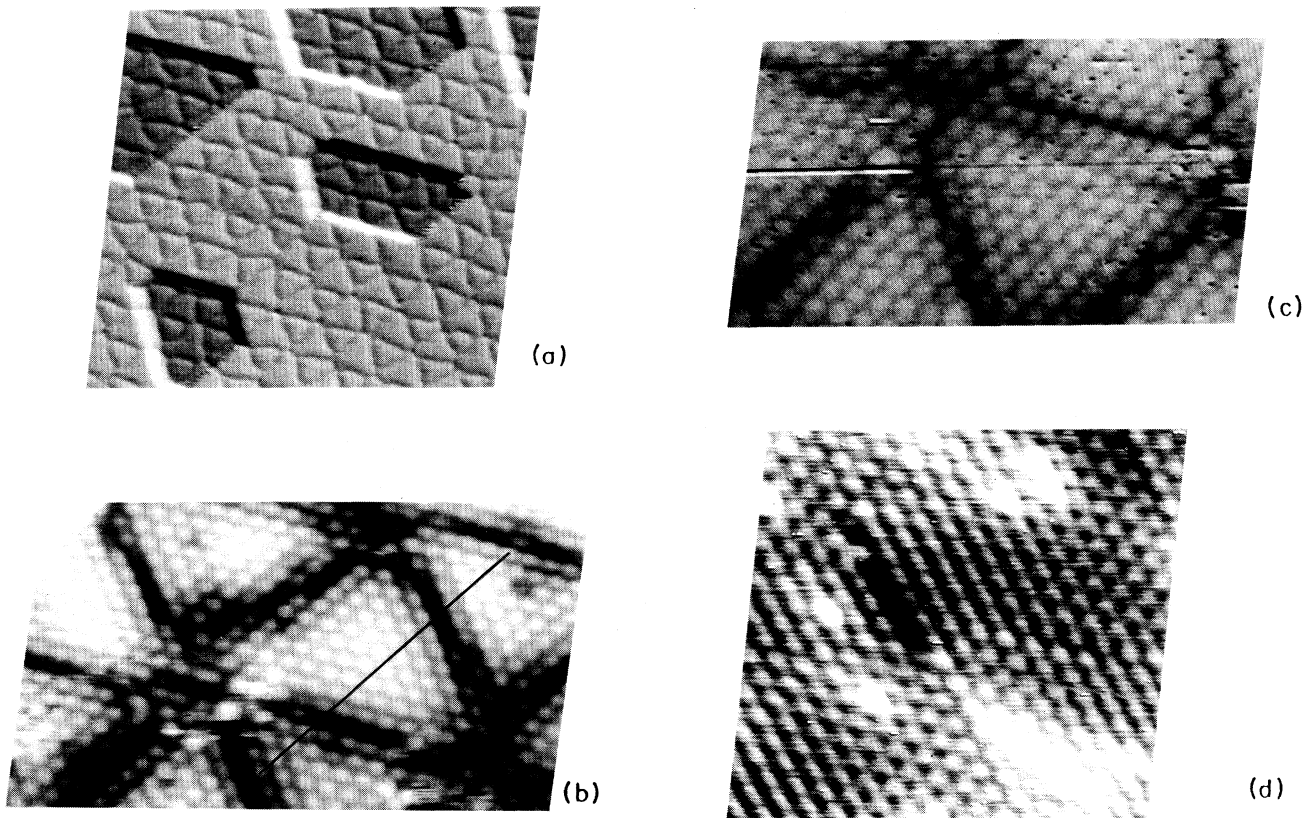


FIG. 2. (a) Domain superlattice of the β phase at 1.0 ML Ga coverage. Two types of domains tile the surface in an alternating way, yielding average trigonal symmetry (deviations from this symmetry are due to meandering of walls). Periodicity of the domain superstructure: ≈ 60 Å. The walls cross substrate steps without lateral shift. $U_g = 2.3$ V, $I_t = 50$ pA, 450 Å \times 450 Å, weighted differential mode. (b) β phase with atomic resolution. Again, the surface atoms in the interior of the domains are in (1×1) geometry, with the lattice constant increased by 8%. A stacking fault is visible in half of the domains. Note the microscopic fluctuation of the walls (lateral shift of the wall line). $U_g = 2.2$ V, $I_t = 20$ nA, 90 Å \times 50 Å. (c) Domain wall of the β phase at positive bias in more detail. One of the walls appears as straight line without meandering. The distances of the surface atoms across the walls are approximately 5.2 Å. $U_g = 2.2$ V, $I_t = 19$ nA, 80 Å \times 45 Å. (d) At negative bias and high I_t (atomic resolution) the domain walls of the β phase are difficult to distinguish and no stacking fault is observed. $U_g = -1.3$ V, $I_t = 11$ nA, 55 Å \times 55 Å, weighted differential mode.

mation calculations on the fully relaxed structure as described in the previous paper.¹ In Fig. 5(a) the integrated LDOS between $E_F - 2.0$ eV and E_F (i.e., occupied states) is shown, and in Fig. 5(b) the integrated density of unoccupied states between E_F and $E_F + 2.0$ eV. In a rough approximation, we assume that at positive U_g all unoccupied surface states between E_F and $E_F + eU_g$ contribute to the tunneling current (neglecting a weighting factor for the effective tunneling barrier⁴), while at negative U_g electrons from all occupied sample states between $E_F - eU_g$ and E_F tunnel into empty tip states. From Fig. 5(a) we conclude, that at positive bias mainly unoccupied p_z -like states localized at the Ga atoms are imaged within the domains of both discommensurate phases [Fig. 1(b)

and Fig. 2(b)]. These unoccupied surface states extend far into the vacuum and exhibit well pronounced maxima of corrugation. No occupied states are associated with the Ga atoms in the energy range ($E_F, E_F - 2.0$ eV). Occupied surface states are mainly localized around the Ge atoms of the lower half of the surface bilayer (Ga-Ge backbonds). These subsurface states are hardly extending into the vacuum region and appear less pronounced in shape than the unoccupied states. This explains the weaker corrugation within the domains observed for negative bias [Figs. 1(c) and 2(d)].

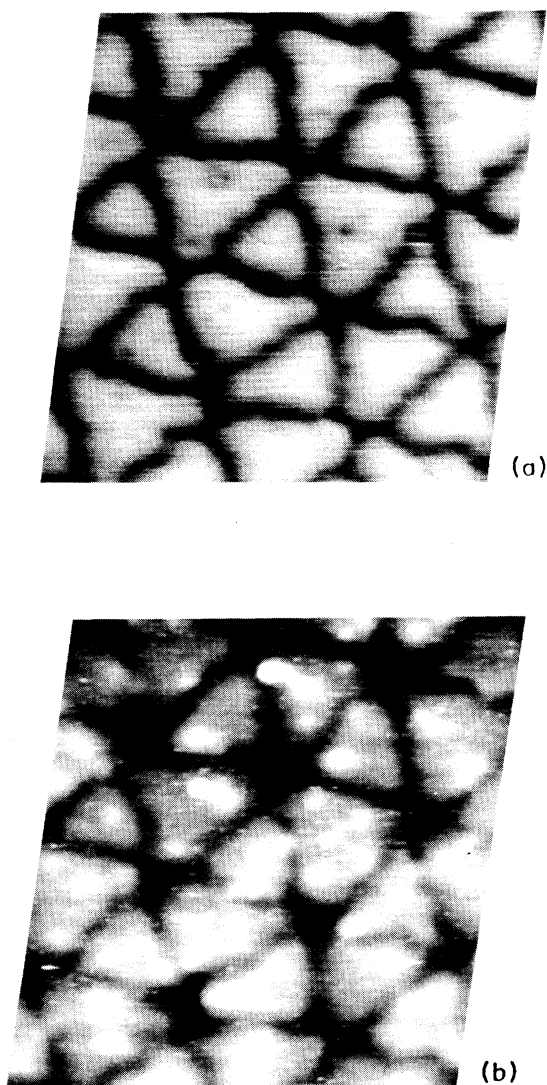


FIG. 3. The same area of a surface covered with the β phase, imaged at positive (a) and negative bias (b) and small I_t . The domain walls are less distinct at negative bias, however they are still clearly visible as minima in the corrugation for small I_t . (a) $U_g = 2.3$ V, (b) $U_g = -2.3$ V, $I_t = 50$ pA, $150 \text{ \AA} \times 170 \text{ \AA}$.

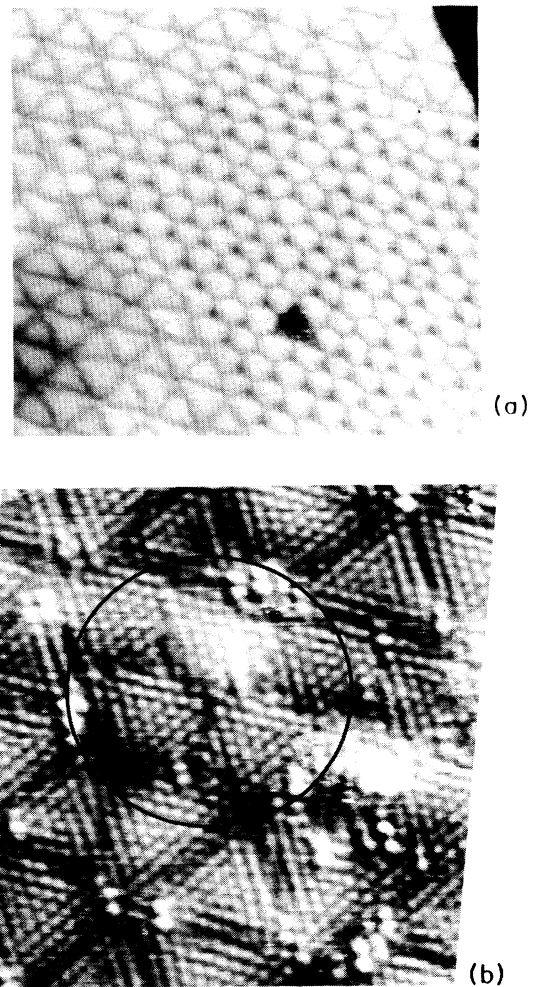


FIG. 4. (a) At the transition value of the Ga chemical potential (Ga coverage between 0.7–0.8 ML) γ and β phase coexist locally. $U_g = 2.4$ V, $I_t = 50$ pA, $400 \text{ \AA} \times 400 \text{ \AA}$, weighted differential mode. (b) A few domains without stacking fault (inside the marked region) embedded in a superlattice of β phase domains. The lattice constants are equal within the resolution of the STM. Although it is not clear whether these domains correspond to an undisturbed γ phase, the image indicates that unfaulted and faulted positions are close in energy and that there is no major change in strain at the transition from γ to β phase. $U_g = 1.0$ V, $I_t = 25$ nA, $150 \text{ \AA} \times 150 \text{ \AA}$, weighted differential mode.

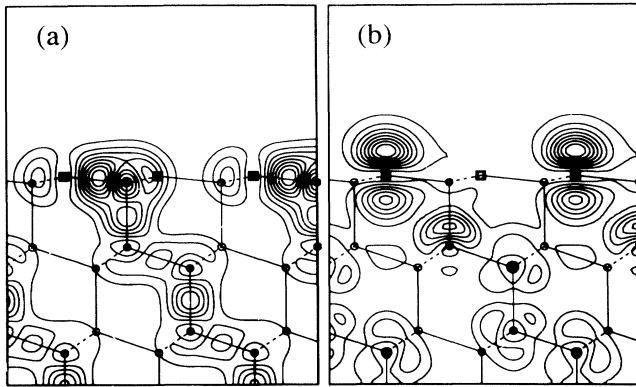


FIG. 5. Contour plots of the local density of electronic states integrated (a) between $E_F - 2.0$ eV and E_F (occupied states) and (b) between E_F and $E_F + 2.0$ eV (unoccupied states), for Ga in substitutional sites in the surface layer. The plots are on $(0\bar{1}1)$ planes. Square symbols indicate Ga atoms, round symbols Ge atoms. Filled symbols denote atoms in the plane to which the contour plot refers. Open circles indicate atoms in a parallel plane distant $a_0/2$ from the previous one, with $a_0 = 4.0$ Å denoting the substrate lattice constant.

A. γ phase

Figure 6 shows a section of a STM image at positive U_g and high current across three adjacent domains of the γ phase along the $\langle 10\bar{1} \rangle$ direction (i.e., along the rows of surface atoms). Within the domains the corrugation due to the surface Ga atoms is about 0.05 Å. Across the domain walls the corrugation increases to more than 0.2 Å.

The equidistant vertical lines mark the corrugation maxima of the domain in the center. Proceeding to the adjacent domains, these lines now coincide with the minima of corrugation. This directly supports a qualitative one-dimensional model of the γ phase deduced from the intensity pattern observed in LEED and surface x-ray diffraction (SXD).² Due to the $\approx 8\%$ mismatched lat-

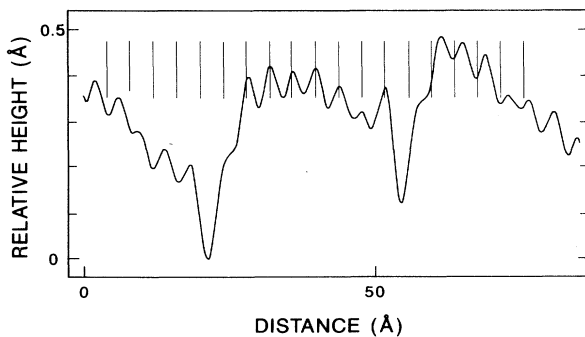


FIG. 6. Section across three adjacent domains of the γ phase along $\langle 10\bar{1} \rangle$ through a row of surface atoms. A convex profile is superposed by the corrugation maxima due to the sites of the Ga atoms. The equidistant vertical lines fall upon the corrugation maxima in the central domain and the minima of the neighboring domains.

tice in the interior of the domains, diffraction intensity is expected at $1.08^{-1} = 0.926$ (in units of the substrate's reciprocal lattice). However, no intensity is observable at this position in LEED and SXD. The extinction of the reflection is readily explained by the assumption of antiphase scattering between neighboring domains. The antiphase condition of the atomic arrangement is revealed by STM as visible in Fig. 6. In addition, this observation allows a simple estimate of the average internal strain (lattice mismatch) without referring to an exact calibration of the length scale of the STM. From LEED and surface x-ray diffraction the average periodicity of the domain superlattice of the γ phase is known to be $7.4 \times a_0 = 29.6$ Å. In a simplified model we assume identical domains with seven atoms. The central atom of each domain is fixed to a regular lattice position, while atoms off the center are shifted away from the regular positions due to the lattice mismatch. This deviation increases with increasing distance from the center until for the fourth atom off the center the strain is so unfavorable, that a domain wall and finally a new domain is formed with the domain wall as symmetry line. Using the antiphase relation between the positions of the atoms of adjacent domains, we obtain the equation $6a'_s + 3/2a''_s = 8a_0 = 32$ Å, with a'_s denoting the lattice constant of the strained surface covered with these domains; thus, $a'_s = 4.26$ Å i.e., 6.5% strain. Similarly, domains with five atoms along the line yield $4a''_s + 3/2a'_s = 6a_0 = 24$ Å, thus $a''_s = 4.36$ Å or 9% mismatch. Finally, the weighted average for a domain superlattice periodicity of 29.6 Å corresponds to an average lattice constant of $a_s = 4.3$ Å or 7.5% strain, i.e., a value slightly lower than determined from XSW (which yields an upper limit of 10%), first-principles calculations (9–10%) as well as direct estimation from STM ($8.0 \pm 3\%$).

In the above calculation, we assumed light walls, i.e., walls with a density of Ga atoms lower than in the interior of the domains. Heavy walls (i.e., elementary discommensurations with a higher density of Ga atoms than within the domains) can be excluded for several reasons. Generally light walls are expected in incommensurate structures for positive mismatch.⁵ In the present system, this is confirmed by several experimental observations. Firstly, the saturation coverage of the γ phase (around 0.7 ML Ga) is lower than expected solely from the increased lattice constant within the domains [$(1.08)^{-2}$ ML = 0.86 ML]. Secondly, the observed change of contrast at the domain walls when changing the polarity of U_g is contrary to that expected for Ga atoms. As mentioned above, a high density of unoccupied states is localized at the Ga atoms, whereas the density of occupied states is low at these sites. Thus, we expect high corrugation at Ga sites when imaging unoccupied states at positive bias and low corrugation at negative bias, which is just the opposite of the observed change in contrast at the domain walls. We conclude that the chemical environment at the domain walls (chemical composition and binding) must be different from the interior of the domains. This will be discussed in more detail in the next section. From the assumption of light walls and using the antiphase relation between atomic positions of adjacent domains, we

obtain a saturation coverage of approximately 0.75 ML Ga in good agreement with the experimentally observed value.

B. β phase

In STM images like Fig. 4(b), we do not find significant differences in the lattice constants or strain for the γ and β phase. The main difference is the presence of a stacking fault in half of the domains of the β phase, giving rise to two inequivalent types of domains, differing in their apparent size and also slightly in their average corrugation [Fig. 2(b)]. Although this information is not directly obtainable from STM, we assume the fault to occur in the smaller domain type because Ga in faulted substitutional positions has a higher energy than in unfaulted positions.¹ Indeed the ratio of the areas of both domain types obtained from STM agrees excellently with the value estimated from XSW (approximately 60% unfaulted, 40% faulted). Most surprisingly, no stacking fault is observable when atomic resolution is achieved at negative bias and high I_t [Fig. 2(d)]. In addition, the domain walls are almost undetectable in this image. However, comparing with Fig. 5(a) one realizes, that the Ga atoms do not provide any density of occupied states up to 2 eV below the Fermi level. Consequently, at negative bias with the tip close enough to the surface the Ga-Ge backbones are imaged [small tip-sample distances are necessary for sufficient overlap of the tip's wave functions with the occupied surface states localized very close to the surface, Fig. 5(b)]. The resolution of the tip is not sufficient to distinguish single bonds, instead corrugation maxima located at the Ge atoms of the second layer are visible—and, consequently no stacking fault is observed. On the contrary, for small I_t , i.e., large tip-sample distance, no significant overlap with the occupied backbone states occurs and the tip's trajectory at negative U_g is mostly determined by a geometric height difference across the walls [Fig. 3(b)].

The additional positive energy contribution due to Ga atoms in faulted positions might be outweighed by an energetically more favorable situation within the domain walls of the β phase. By comparison of Fig. 2(b) and (d) with the corresponding images for the γ phase [Fig. 1(b) and (c), respectively], we indeed find a distinct difference between both types of domain walls. Contrary to the γ phase, no contrast reversal is observed for the β phase when changing the polarity of the tunneling bias. Instead the walls appear less distinct or even undetectable at negative bias. From this we propose that within the walls of the β phase, most dangling bonds are saturated, in contrast to the situation in the domain walls of the γ phase. Again we assume, that at negative bias within the domains of the γ -phase Ge atoms (more correct: the occupied Ga-Ge backbones) in the second layer are imaged. Most of the corrugation maxima in the walls fall upon the lines defined by the rows of these Ge atoms in the domains along the $\langle 10\bar{1} \rangle$ directions. Thus, we tentatively interpret the corrugation maxima within the walls of the

γ phase as unsaturated dangling bonds of Ge atoms in the second layer. The introduction of a stacking fault in the β phase allows a more favorable binding situation of atoms within the domain walls and the passivation of all

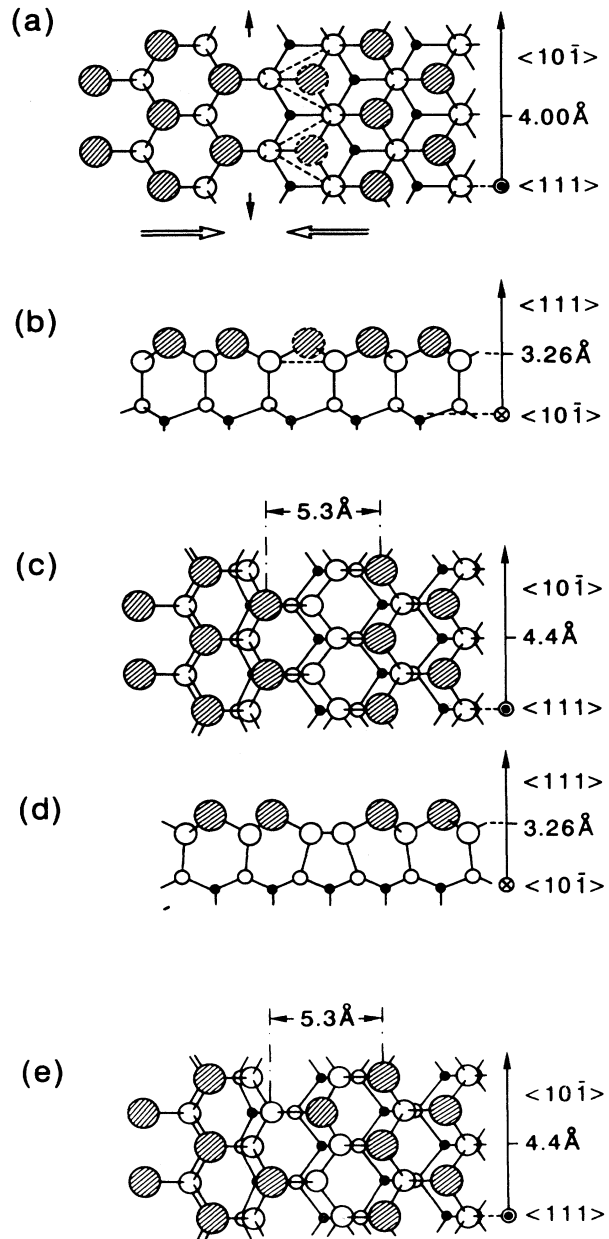


FIG. 7. Model for the domain walls of the β phase. (a) Within the walls a row of substitutional Ga atoms is missing (dotted filled circles), resulting in dangling bonds located at Ge atoms in the second layer. Due to the $\approx 9\%$ lattice mismatch the domains extend laterally. The atoms at the edges of adjacent domains move by ≈ 1.4 Å perpendicular to the wall (large arrows), until the distance of the second-layer Ge atoms across the wall corresponds to the usual Ge-Ge bond length. (b) Side view of (a). (c) The dangling bonds are saturated by the formation of a zigzag chain of covalently bonded Ge atoms along $\langle 10\bar{1} \rangle$ in the second layer. (d) Side view of (c). (e) Microscopic model for the meandering of domain walls.

dangling bonds. The accompanied gain in energy overcompensates the loss due to the stacking fault. It allows a more compact packing of Ga atoms in the domain walls and thus accounts for the higher saturation coverage of the β phase.

C. Model for the domain wall of the β phase

From Fig. 1(c), it is obvious that the binding configuration at the domain walls of the γ phase is rather complicated. Up to now, it was not possible to deduce a satisfying model for these walls and they may, in fact, not even possess a well defined structure. Contrary to the γ phase, the walls in the β phase appear much more regular [Fig. 2(c)]. An acceptable model of these walls should fulfill the following conditions.

(i) It has to include the observed stacking fault and the lattice mismatch.

(ii) The walls have to be light and the atomic distances across the walls determined with STM should be reproduced.

(iii) The dangling bonds should be saturated within the walls.

(iv) The model should account for the meandering of the walls.

A model which fulfills all these requirements is shown in Fig. 7. A row of substitutional Ga atoms is missing within the walls [dotted in Fig. 7(a)]. The thus produced dangling bonds of the Ge atoms in the lower half of the surface bilayer are saturated by the formation of a zig-zag chain of covalently bound Ge atoms along $\langle 10\bar{1} \rangle$ within this layer. In Fig. 7(a), the distance of the corresponding Ge atoms is too large for covalent bonds to be formed. However, due to the lattice expansion within the domains, adjacent domains move laterally in the direction perpendicular to the wall until the distance of the Ge atoms with dangling bonds is $\approx 2.4 \text{ \AA}$, i.e., the length of a usual covalent Ge-Ge bond. To simplify the present discussion we assume unfaulted and faulted domains of equal size with the central atom of each domain fixed laterally to a regular substrate lattice site. Isotropic increase of the lattice constant by 9% results in the geometry depicted in Fig. 7(c), where the atoms at the edges of the domains moved $\approx 1.4 \text{ \AA}$ in the direction perpendicular to $\langle 10\bar{1} \rangle$ and the distance of the second-layer Ge atoms within the wall is $\approx 2.4 \text{ \AA}$. The distance of the Ga atoms across the domain walls is 5.3 \AA in agreement with the value obtained from STM ($5.2 \text{ \AA} \pm 0.3 \text{ \AA}$).

Figure 7(e) shows, that the model can also account for the fluctuation of the domain walls. It is interesting to realize, that in this model the meandering does not cost any chemical energy (instead only minor energetic contributions due to altered strain) and thus might be an entropy-driven effect. The fluctuations of the walls occurring at the high formation temperatures of the β phase (typically annealing temperatures around 500°C)

may be frozen during the cooling of the samples investigated here. The slightly different morphology of the domain walls observed, e.g., when comparing Fig. 2(b) and (c), may be the result of a slightly different annealing temperature and/or cooling procedure. It might be an interesting future project to investigate the domain walls with STM at different (especially higher) temperatures or at least for different preparation procedures (e.g., extremely slow cooling).

We note that the increasing bending of bonds between Ge atoms of the second and the third layer with increasing distance from the center of the domains leads to a convex profile of the surface of the domains, if we assume constant length of these bonds. This may result in the observed profile shown for the γ domains in STM Fig. 6. One might expect that with increasing distance from the center the increasing bending of these bonds should result in an enhanced force acting on the surface atoms pulling them towards the center of the domains. This could produce an inhomogeneity in the strain, with smaller mismatch at the edges of the domains than in the center. If such an inhomogeneity in strain for the β as well as the γ phase exists, it is beyond the resolution of our STM. Recently obtained SXD data on both phases however might indicate the expected inhomogeneity in strain.⁶

V. SUMMARY

In summary, the STM data support the results which were obtained in part I via *ab initio* calculations and XSW measurements and provide information about the structure at the domain walls. Within the domains of the γ and the β phase of Ge(111)/Ga, substitutional Ga atoms are essentially in (1×1) geometry with a lattice constant increased by $\approx 8\%$ with respect to the substrate due to large adsorbate induced compressive strain. In the β phase a stacking fault is observed in half of the domains. While within the domain walls of the γ phase unsaturated dangling bonds are present, the stacking fault in the β phase allows a binding configuration within the walls, where all dangling bonds are removed. The accompanied gain in energy exceeds the loss in energy due to the partial stacking fault. Thus an altered binding in the domain walls is the main driving force for the transition from the γ to the β phase.

ACKNOWLEDGMENTS

Skillful technical assistance by W. Stiepany is gratefully acknowledged. E. A. acknowledges financial support by the Alexander von Humboldt foundation.

* Present address: Institut de Physique Experimentale, Université de Lausanne, CH-1015 Lausanne, Switzerland.

† Author to whom all correspondence should be addressed.

¹ E. Artacho, P. Molinàs-Mata, M. Böhringer, J. Zegenhagen, G. Franklin, and J. R. Patel, preceding paper, Phys. Rev. B **51**, 9952 (1995).

² P. Molinàs-Mata, M. Böhringer, E. Artacho, J. Zegenhagen, L. Seehofer, T. Buslaps, R. L. Johnson, E. Findeisen, R. Feidenhans'l, and M. Nielsen, Phys. Status Solidi (to be published).

³ Omicron Vakuumphysik, Taunusstein, Germany.

⁴ See, e.g., R. M. Tromp, J. Phys. Condens. Matter **1**, 10211 (1989), and references therein.

⁵ See, e.g., P. Bak, in *Chemistry and Physics of Solid Surfaces V*, edited by R. Vanselow and R. Howe (Springer-Verlag, Heidelberg, 1984).

⁶ J. Zegenhagen, M. Böhringer, R. Feidenhans'l, G. Falkenberg, L. Seehofer, L. Lottermoser, and R.L. Johnson (unpublished).

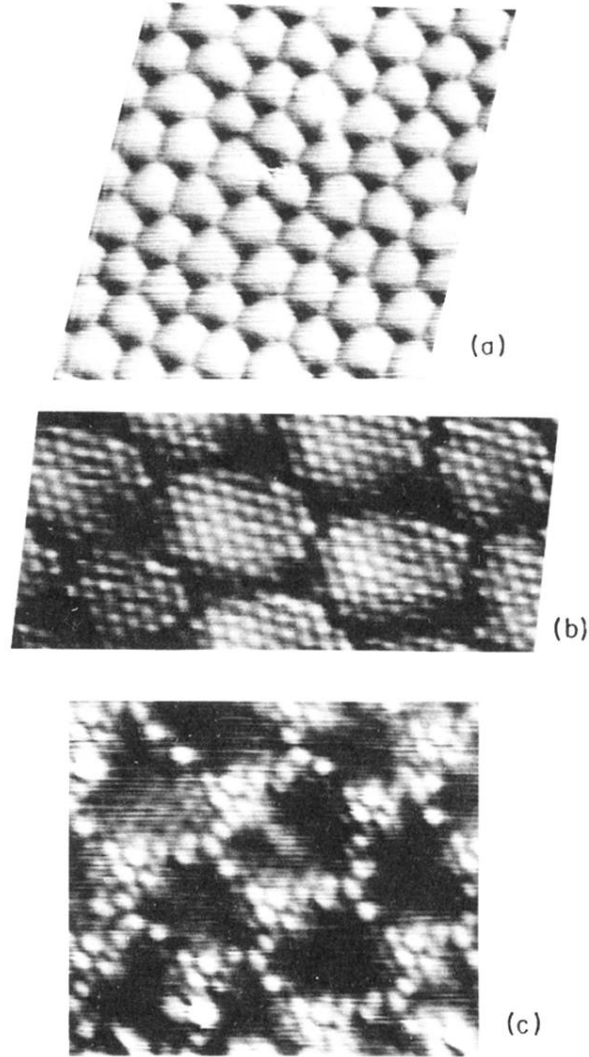


FIG. 1. (a) Domain superlattice of the γ phase at 0.6 ML Ga coverage. The periodicity of the superstructure is $\approx 30 \text{ \AA}$. Two types of wall intersections are visible, leading to trigonal rather than hexagonal symmetry. $U_g = 2.5 \text{ V}$, $I_t = 50 \text{ pA}$, $200 \text{ \AA} \times 200 \text{ \AA}$, weighted differential mode. (b) High resolution STM constant current topograph (CCT) of the domains of the γ phase. Within the domains the surface atoms are in (1×1) geometry with a lattice constant increased by $\approx 8\%$ with respect to the bulk (4.3 \AA and 4.0 \AA , respectively). $U_g = 2.2 \text{ V}$, $I_t = 23 \text{ nA}$, $100 \text{ \AA} \times 45 \text{ \AA}$, weighted differential mode. (c) At negative bias, corrugation maxima are visible within the domain walls, most probably originating from dangling bonds in the second layer. Note the triangular arrangement of maxima at every second wall intersection. $U_g = -2.5 \text{ V}$, $I_t = 2.9 \text{ nA}$, $90 \text{ \AA} \times 90 \text{ \AA}$, weighted differential mode.

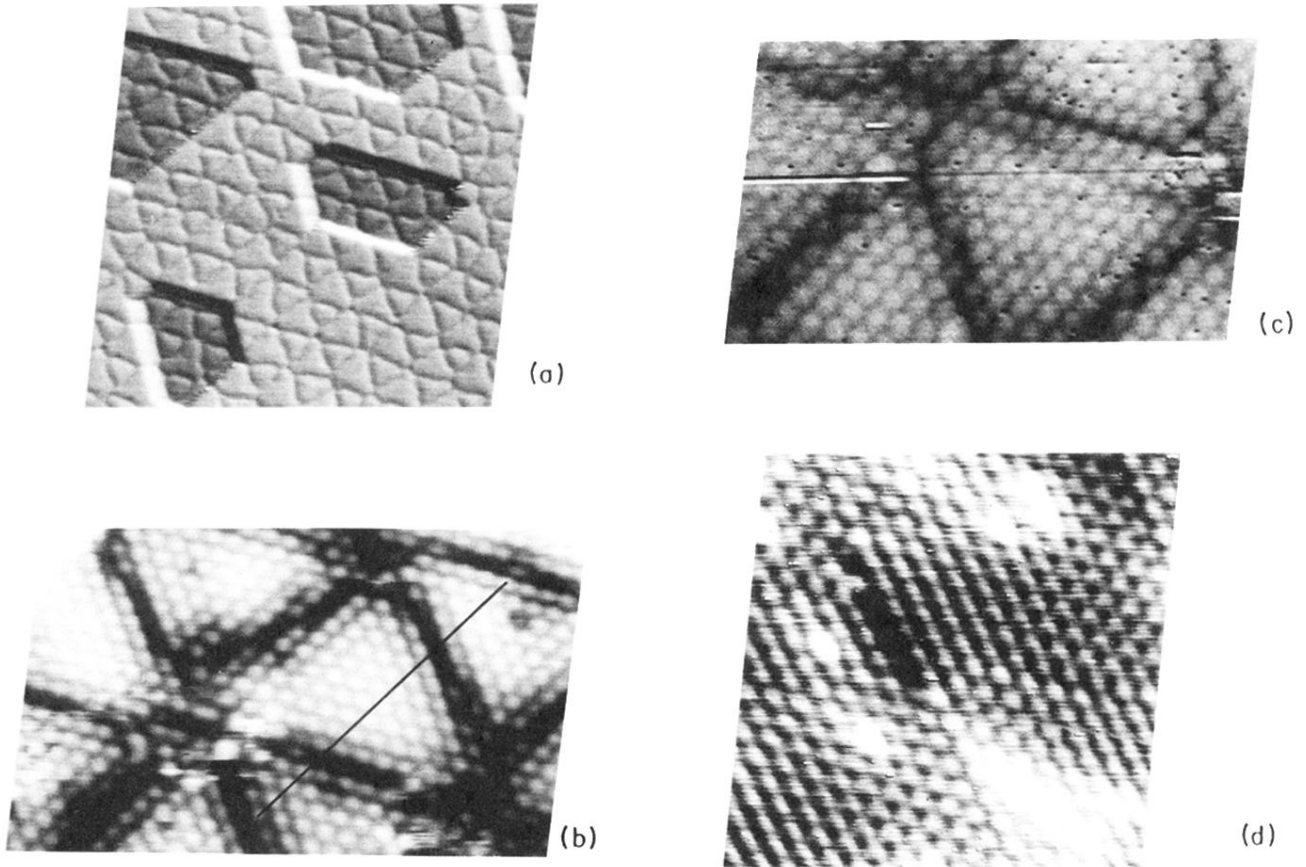
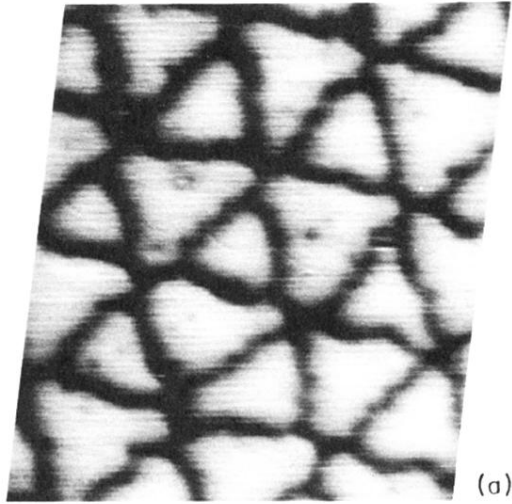
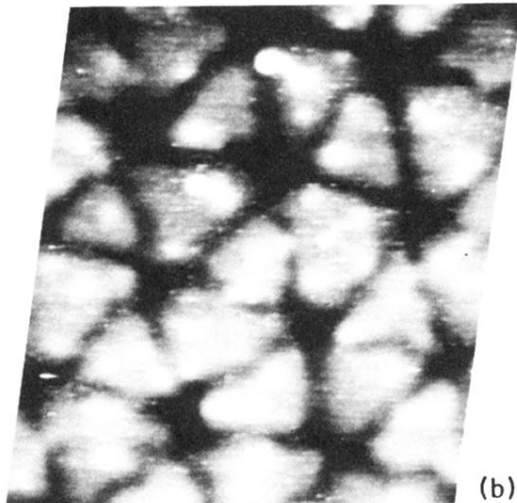


FIG. 2. (a) Domain superlattice of the β phase at 1.0 ML Ga coverage. Two types of domains tile the surface in an alternating way, yielding average trigonal symmetry (deviations from this symmetry are due to meandering of walls). Periodicity of the domain superstructure: $\approx 60 \text{ \AA}$. The walls cross substrate steps without lateral shift. $U_g = 2.3 \text{ V}$, $I_t = 50 \text{ pA}$, $450 \text{ \AA} \times 450 \text{ \AA}$, weighted differential mode. (b) β phase with atomic resolution. Again, the surface atoms in the interior of the domains are in (1×1) geometry, with the lattice constant increased by 8%. A stacking fault is visible in half of the domains. Note the microscopic fluctuation of the walls (lateral shift of the wall line). $U_g = 2.2 \text{ V}$, $I_t = 20 \text{ nA}$, $90 \text{ \AA} \times 50 \text{ \AA}$. (c) Domain wall of the β phase at positive bias in more detail. One of the walls appears as straight line without meandering. The distances of the surface atoms across the walls are approximately 5.2 \AA . $U_g = 2.2 \text{ V}$, $I_t = 19 \text{ nA}$, $80 \text{ \AA} \times 45 \text{ \AA}$. (d) At negative bias and high I_t (atomic resolution) the domain walls of the β phase are difficult to distinguish and no stacking fault is observed. $U_g = -1.3 \text{ V}$, $I_t = 11 \text{ nA}$, $55 \text{ \AA} \times 55 \text{ \AA}$, weighted differential mode.

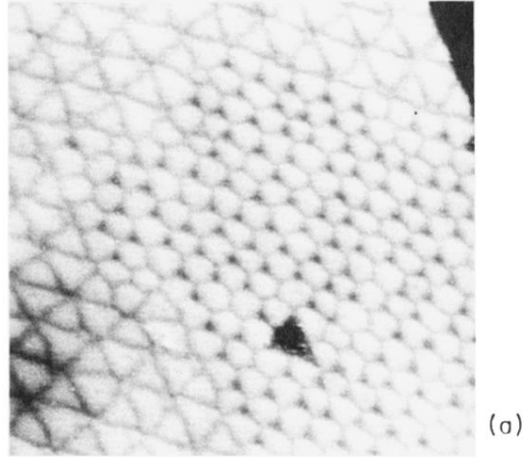


(a)

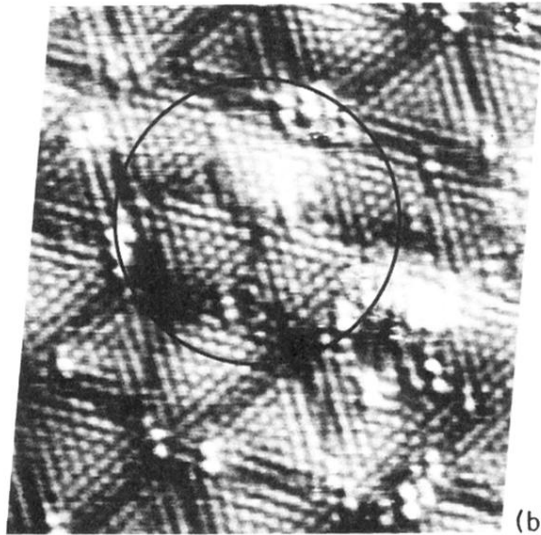


(b)

FIG. 3. The same area of a surface covered with the β phase, imaged at positive (a) and negative bias (b) and small I_t . The domain walls are less distinct at negative bias, however they are still clearly visible as minima in the corrugation for small I_t . (a) $U_g = 2.3$ V, (b) $U_g = -2.3$ V, $I_t = 50$ pA, $150 \text{ \AA} \times 170 \text{ \AA}$.



(a)



(b)

FIG. 4. (a) At the transition value of the Ga chemical potential (Ga coverage between 0.7–0.8 ML) γ and β phase coexist locally. $U_g = 2.4$ V, $I_t = 50$ pA, $400 \text{ \AA} \times 400 \text{ \AA}$, weighted differential mode. (b) A few domains without stacking fault (inside the marked region) embedded in a superlattice of β phase domains. The lattice constants are equal within the resolution of the STM. Although it is not clear whether these domains correspond to an undisturbed γ phase, the image indicates that unfaulted and faulted positions are close in energy and that there is no major change in strain at the transition from γ to β phase. $U_g = 1.0$ V, $I_t = 25$ nA, $150 \text{ \AA} \times 150 \text{ \AA}$, weighted differential mode.